EFFICACY OF SILVER IBUPROFEN AGAINST BACTERIAL SKIN PATHOGENS: A POTENTIAL TREATMENT FOR SURGICAL SITE INFECTIONS.

An Undergraduate Research Scholars Thesis

by

MORGAN JAMES CHAPMAN

Submitted to the Undergraduate Research Scholars program at
Texas A&M University
in partial fulfillment of the requirements for the designation as an

UNDERGRADUATE RESEARCH SCHOLAR

Approved by Research Advisor: Dr. Carolyn L. Cannon M.D., Ph.D.

May 2019

Major: Microbiology
Genetics

TABLE OF CONTENTS

ABSTRACT

Coaxially Electrospun Nanofibers as a Drug Delivery System for Silver Ibuprofen to Surgical Site Infections

Morgan James Chapman
Department of Biology
Texas A&M University

Research Advisor: Dr. Carolyn L. Cannon M.D., Ph.D.
Department of Microbial Pathogenesis and Immunology
Texas A&M University Health Science Center

Each year, hundreds of thousands of Americans are affected by surgical site infections (SSIs), resulting in billions of dollars spent on additional healthcare and thousands of lives lost. These SSIs are often caused by *Pseudomonas aeruginosa, Staphylococcus epidermidis,* and methicillin resistant *Staphylococcus aureus* (MRSA), opportunistic pathogenic bacteria present in the skin flora. During surgeries, the site of incision traditionally maintains its sterility through the use of hygienic practice and chemicals. However, sterility may be compromised due to the intercalation of pathogenic bacteria into the site of incision from the crevasses of the skin thus leading to infection. Due to the secretory nature of wound sites, it is possible to use an elution-based delivery system for the direct and continuous delivery of silver ibuprofen (AgIBU), a potent antimicrobial with anti-inflammatory effects. Using electrospinning techniques, nanofiber scaffolds loaded with AgIBU were constructed and subjected to release studies. Results displayed drug release significantly higher than needed to inhibit clinical strains of *P. aeruginosa, S. epidermidis,* and MRSA. Thus, AgIBU based nanofiber-elution therapy may allow for the direct and continuous treatment of pathogenic bacteria in the skin flora, reducing SSIs and inflammation at wound sites.

DEDICATION

I would like to thank my principle investigator, Dr. Carolyn L. Cannon, postdoctoral fellow, Dr. Kush N. Shah, graduate student, Bhagath Chirra, and research assistant, Sabona B. Simbassa for their mentorship, guidance, and support over the course of this project, they provided me with the tools to succeed and helped make this project a wonderful experience.

I would also like to extend my gratitude to my team who have dedicated so much of their time to me and being invaluable, thank you, Jaime Baez, Adel H. Hassan, Ahmed Basharat, Francisco Torres, and Tristan Estrada.

Finally, I would like to extend thanks to my family; Kenda Thurmond, Steve Thurmond, and Marie Bolt. Your support, patience, and encouragement have been huge factors in my success in completing this project, thank you.

ACKNOWLEDGEMENTS

I would like to thank the Cannon lab for their immense support and hard-work on all aspects of this project, from antimicrobial susceptibility studies to cytotoxicity studies, none of it could be done without you. Thank you to my lab mates, Qingquan Chen, Sabona B. Simbassa, Chelsea M. Ebert, Jeremiah A. Alexander, Rohit Raina, Marita John, and Marleini Ilanga.

I would also like to thank Samuel Briggs and the Maitland Lab for sharing their equipment and time. Their generosity was immense in the completion of this project.

NOMENCLATURE

ACN	Acetonitrile
AgIBU	Silver Ibuprofen
ACDR	Average Cumulative Drug Release
Bug	Bacterial strain
C	Celsius
CFU	Colony Forming Units
CHCl3	Chloroform
cm	Centimeter
DIW	DeIonized Water
DMSO	Dimethyl Sulfoxide
HFIP	Hexafluoro-2-propanol
IS	Initial Stock
μg	Microgram
mg	Milligram
mL	Milliliter
mm	Millimeter
M	Molar, moles per liter
MBC	Minimum Bactericidal Concentration
MHB	Mueller Hinton Broth
MIC	Minimum Inhibitory Concentration
PBSoln	Phosphate Buffer Solution
PC	Positive Control
PCL	Polycaprolactone
Rpm	Revolutions per minute
SEM	Scanning Electron Microscope
Soln	Solution
SSI	Surgical Site Infection
TCDR	Total Cumulative Drug Release
TSA	Tryptic Soy Agar
WS	Working Stock

CHAPTER I

INTRODUCTION

Each year in the United States, there are an estimated 160,000-300,000 cases of surgical site infections (SSIs) costing the healthcare system between $3.5 billion and $10 billion annually [1]. Of these SSIs, 60% are estimated to be preventable and increase the chance of mortality in patients' 2 to 11 fold [2]. Many of these infections are attributed to strains belonging to the bacterial species *Pseudomonas aeruginosa*, a Gram-negative rod, and *Staphylococcus epidermidis* and *Staphylococcus aureus,* both Gram-positive cocci, all of which are opportunistic pathogenic bacteria prevalent in the skin flora [3]. Traditional treatments to prevent these infections have been hygienic surgical practice and thorough sterilization of equipment. However, with the discovery of antibiotics, traditional and new therapies have been combined to develop more effective techniques to mitigate these nosocomial infections.

Despite these practices, rates of SSIs have continued to rise due to the sharp increase in the number of multidrug resistant (MDR) bacteria, a product of the abuse and misuse of antibiotics [4]. Consistent misuse of antimicrobials in conjunction with horizontal gene transfer has led to the proliferative acquisition of resistant genes in pathogenic bacterial communities, reducing the efficacy of many standard of care antibiotics. To worsen the problem, many large pharmaceutical companies have abandoned research and development of antibiotic due to the high cost and low percentage of FDA-approval [5]. The decrease in the development of FDA-approved antimicrobials combined with the rapid increase of MDR bacteria including MDR-*P. aeruginosa* and methicillin resistant *S. aureus* (MRSA) has led to the critical need for the development of non-toxic, broad-spectrum antimicrobials.

With this in mind, we looked at the cooperative use of two common FDA-approved agents to create a new, broad-spectrum antimicrobial; silver and ibuprofen. Silver was of interest to us because of its antibacterial properties, and routine use for sterilization of medical equipment, and the treatment of burn wound infections. Silver has antibacterial activity while in its Ag^{+1} oxidation state due to its ability to bind negatively charged macromolecules, disrupt cellular membranes, and produce reactive oxidative species [6]. These multiple modes of action contribute to silver's biocidal effects in both Gram-positive and Gram-negative bacteria, and to its antimicrobial efficacy at low concentrations [7]. Complementing its oligodynamic effects, silver is readily reused within a bacterial population leading to a "zombie" effect where bacteria exposed to silver release the ion into the proximity of other bacteria upon lysis [8]. This secondary release from lysing bacteria allows for silver to be used over and over again within a bacterial population, improving its antimicrobial efficacy, and potentially, improving its time to act against a bacterial infection. In addition to acting against bacteria, heavy metals such as silver have been shown to induce cytotoxicity in human cells. However, through the use of antioxidants, the toxic effects against human cells can be abrogated [9]. For example, silver demonstrates toxic effects in human dermal fibroblasts; however, Raina et al. observed that when preincubated with N-acetyl cysteine, an antioxidant and precursor to glutathione, silver-exposed cells demonstrate cytotoxic effects only at high silver concentrations, and no cytotoxic effects at silver concentrations sufficient to kill bacteria [10].

Ibuprofen, a common nonsteroidal anti-inflammatory drug, was considered for use in our antibiotic therapies to address the inflammation associated with SSIs. A clinical study demonstrated that treatment with high dose oral ibuprofen impressively improves the lung function in cystic fibrosis patients [11]. At the time, improvement in lung function was thought

to be due solely to the anti-inflammatory effects of ibuprofen; however, under closer examination, we demonstrated that ibuprofen has mild antimicrobial properties of its own against bacterial species such as *P. aeruginosa* and MRSA [12]. In addition to its antimicrobial activity, we observed that ibuprofen also displays synergistic properties, improving the efficacy of standard of care antibiotics. These novel properties of ibuprofen to synergize with already-effective antimicrobials and to act as an anti-inflammatory were the basis for the development of silver ibuprofen, a silver salt with potent, broad-spectrum antimicrobial activity.

Because silver ibuprofen is only soluble in organic solvents, a delivery system was necessary to guide the drug to the site of infection. Previous studies in drug-delivery have illustrated the use of electrospun nanofibers as a method of delivery due to their ease of fabrication and biodegradable properties [13-16]. Using polycaprolactone (PCL) as a structural polymer, nanofiber scaffolds laced with silver ibuprofen may be fabricated via electrospinning. The release of loaded compounds from nanofiber scaffolds is caused by the degradation reaction of the structural polymer, a hydrolysis reaction initiated by the interaction of water with nanofibers [13,14]. Although slightly hydrophilic, PCL does not readily associate with water and in turn does not readily elute silver ibuprofen. Amphiphilic compounds, such as polyethylene glycol (PEG), can associate with PCL in the structural component of the nanofibers while also serving as a hydrophilic island for water to readily associate with and initiate the degradation reaction [16]. Elution based therapy from nanofiber scaffolds provides direct and continuous delivery of silver ibuprofen at the site of wound infection potentially maintaining sterility and decreasing inflammation.

CHAPTER II

METHODS

Materials

Chemical Compounds

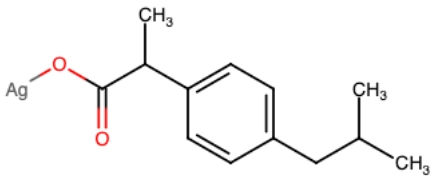

Figure 1. Chemical structure of silver ibuprofen.

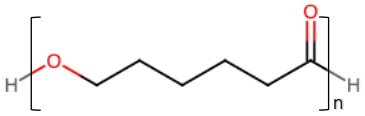

Figure 2. Chemical structure of polycaprolactone

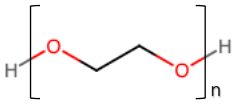

Figure 3. Chemical structure of polyethylene glycol.

Silver ibuprofen (**Fig. 1)**, the therapeutic of interest, was loaded into electrospun nanofibers composed of 80,000 Dalton polycaprolactone chain lengths **(Fig 2)**. Nanofibers were doped with 2,000 Dalton polyethylene glycol chain lengths (**Fig. 3)** to increase the hydrophilicity of the fibers and improve the release of silver ibuprofen.

Preparation of phosphate buffer solution

In order to quantify the cumulative AgIBU release and rate of release from the nanofiber scaffolds, a phosphate buffer solution (PBSoln) was prepared at physiological pH (7.4). The solution was composed of 40.5mL of 0.2M sodium phosphate dibasic heptahydrate and 9.5mL of 0.2M sodium phosphate monobasic monohydrate.

Synthesis of Silver Ibuprofen (AgIBU)

The silver salt of ibuprofen was synthesized using a precipitation reaction utilizing equimolar concentrations of silver nitrate and the sodium salt of ibuprofen, both dissolved in water. The reaction proceeded for 30 minutes while being constantly stirred in a flask protected from light. The AgIBU precipitates were then filtered and washed with water, removing any excess sodium nitrate, before being flash frozen and lyophilized to constant weight. The final product was subjected to analysis by Hydrogen-1 Nuclear Magnetic Resonance (H^1-NMR) and mass spectrometry.

Bacterial Strains

Clinical isolates of *Pseudomonas aeruginosa* isolates, including multi-drug resistant (MDR)-*P. aeruginosa, Staphylococcus epidermidis,* and methicillin resistant *Staphylococcus aureus* (MRSA) were isolated from cystic fibrosis of patients when under the care of Dr. Carolyn L. Cannon at St. Louis Children's Hospital or acquired from BEI resources. The antimicrobial activity of AgIBU was determined against 22 *P. aeruginosa*, including MDR-*P. aeruginosa* in **Table I**, 16 *S. epidermidis* **Table II** and 45 MRSA isolates in **Table III**.

Culturing Bacterial Strains

Single colony purification of the bacterial strains from **Tables I-III** were conducted by streaking onto tryptic soy agar (TSA) plates and incubated at 37ºC for 18-24 hours. Broth cultures were prepared by inoculating a 5mL of Mueller Hinton Broth (MHB) with a single colony and cultured to a log-phase growth (OD_{650nm}=0.4) in incubator with constant shaking at 200 rpm at 37ºC. Bacterial inoculums were prepared by diluting down to 5E5 CFU/mL and 100µL were then seeded in triplicates in a 96-microtiter plate resulting in 5E4 CFU/well.

Table I. *Pseudomonas aeruginosa,* including MDR-*P. aeruginosa,* strains list

PA01	PA B2-72
PAM57-15	PA 5-45
PA14	PA 0531
PAHP3	PA 0540
PA 2-39	PA 554
PA 3-13	PA 551
PA 2-31	PA 557
PA 3-2	PA 562
PA 2-68	PA B2-51
PA 2-87	PA 2-40
PA 2-52	PA 2-9

Table II. *Staphylococcus epidermidis* strains list

NRS8 (HIP4680)	NIHLM015
NRS858 (VCU071)	NIHLM031
NRS122	NIH04008
NIHLM067	NRS6 (HIP04645)
NIHLM020	NRS53
NIHLM001	NRS60
NIHLM003	NRS848 (VCU013)
NIHLM008	NRS849 (VCU014)

Table III. Methicillin resistant *Staphylococcus aureus* strains list

USA 300	MRSA 0628
SAD05	MRSA 0631
SAEH06	MRSA 0632
MRSA 0601	MRSA 0633
MRSA 0602	MRSA 0634
MRSA 0604	MRSA 0636
MRSA 0605	MRSA 0638
MRSA 0606	MRSA 0639
MRSA 0607	MRSA 0640
MRSA 0608	MRSA 0641
MRSA 0609	MRSA 0644
MRSA 0610	MRSA 0645
MRSA 0611	MRSA 0646
MRSA 0612	MRSA 2106
MRSA 0613	MRSA 29466
MRSA 0615	MRSA 31225
MRSA 0616	MRSA 30560
MRSA 0617	MRSA 31258
MRSA 0618	MRSA 13566
MRSA 0619	MRSA 30476
MRSA 0621	MRSA 30242
MRSA 0622	MRSA 27630
MRSA 0627	

Antimicrobial Susceptibility Assay

The antimicrobial activity of AgIBU was determined in accordance with the Clinical Laboratory Standard Institute (CLSI) broth microdilution technique. First, a serial dilution of AgIBU with 5% of the solvent dimethyl sulfoxide (DMSO, v/v) was prepared as seen in **Table IV**. Next, a drug gradient in a 96-well plate was prepared using 100µL of the diluted culture in MHB prepared earlier, plus 100µL of each of the AgIBU dilutions in triplicate (**Fig. 4**). A 200µL aliquot of MHB was used as a negative control; the positive control (PC) was comprised of 100µL of the diluted culture and 100µL of MHB with 2.5% DMSO (v/v). The 96-well plate were then sealed with gas permeable Breathe-Easy® membranes and incubated for 18 to 24hr at 37°C. The MIC was determined as the lowest AgIBU concentration with no visible growth. A 100µL solution from the clear wells with no visible growth was plated onto 5% blood agar plates and incubated for 18 to 24 hrs at 37°C to determine the minimum bactericidal concentration (MBC).

Table IV. MIC/MBC Drug Solution Preparation Table

Solution	Initial Concentration of AgIBU (μg/mL)	Final Concentration AgIBU (μg/mL)	Stock	Volume of stock solution (μL)	Volume of DMSO (μL)	Volume of 1M MHB (μL)	Final Volume (μL)
1	0.25	0.125	2	3.125	46.875	950	1000
2	0.50	0.25	2	6.25	43.75	950	1000
3	1	0.5	2	12.5	37.5	950	1000
4	2	1	2	25	25	950	1000
5	4	2	2	50	0	950	1000
6	8	4	1	6.25	43.75	950	1000
7	12	6	1	9.375	40.625	950	1000
8	16	8	1	12.5	37.5	950	1000
9	24	12	1	18.75	31.25	950	1000
10	32	16	1	25	25	950	1000
11	48	24	1	37.5	12.5	950	1000
12	64	32	1	50	0	950	1000

Note: Initial Stock: 10mg/mL, AgIBU in DMSO. Stock 1: 1280 μg/mL, AgIBU in DMSO. 64μL IS and 436μL DMSO. Stock 2: 80 μg/mL, AgIBU in DMSO. 31.25μL Stock 1 and 468.75μL DMSO.

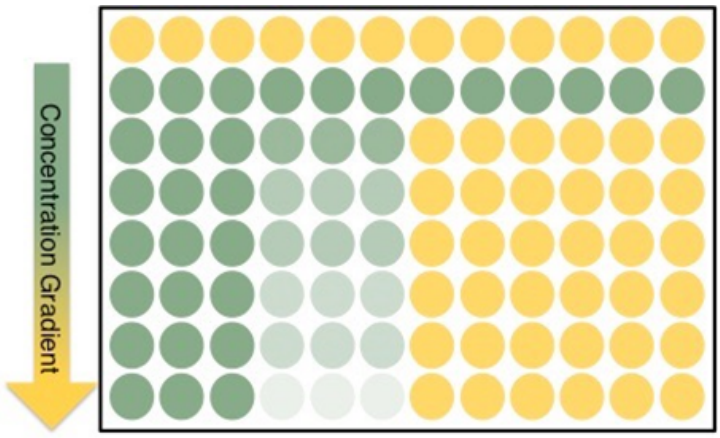

Figure 4. AgIBU Concentration Gradient

Electrospinning

Nanofibers were produced using electrospinning techniques for the direct and continuous elution and delivery of AgIBU to the site of infection **(Fig. 5).** Nanofibers were fabricated using two polymer solutions; composed of a 3:1 ratio of PCL to PEG, each dissolved in chloroform

($CHCl_3$) at 100mg/mL. The drug solution was prepared by dissolving AgIBU in hexafluoro-2-isopropanol (HFIP) at 100mg/mL. Nanofiber scaffold compositions were adjusted to optimize loading efficiency, release rate, and average cumulative drug release. These compositions were, by mass percentage, 80% polymer solution: 20% AgIBU and 90% polymer solution: 10% AgIBU. Nanofiber solutions were dispensed at 2.25 mL/hour flow rate using 15kV with a static grounding plate 10 inches vertically below the spinneret. In addition to AgIBU-loaded scaffolds, unloaded scaffolds were produced as controls, using blank HFIP in electrospinning solutions. After formation, the nanofiber scaffold was stored in a vacuum oven at -22 InHg for 24 hours before being subjected to loading and release studies.

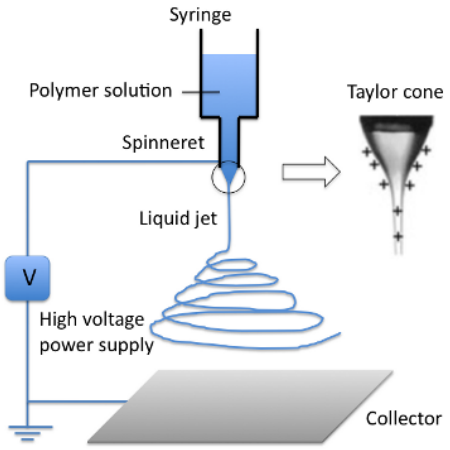

Figure 5. Working principle for electrospinning diagram, Athira et al. 2014.

The nanofibers were characterized using a tabletop Scanning Electron Microscope, observing the differences in structure and nanofiber formation between unloaded and AgIBU-loaded nanofibers. Characterization allowed for the determination of diameter of the nanofibers as well as further confirmation of the presence of AgIBU deposits in the nanofibers.

Loading Study

15mg samples of AgIBU-loaded scaffold were suspended in $CHCl_3$ and DMSO at a 3:1 ratio respectively, dissolving the polymers and releasing any loaded AgIBU. To account for any absorbance by the polymers, controls were prepared using equal weight of unloaded scaffold sample. All samples were analyzed via Cytation 5 Plate Reader at 260nm and compared to the standard curve in **Table V**. Using Beer's Law **Formula 1**, the concentrations of AgIBU present in each of the scaffolds were calculated.

Formula 1. Beer's Law $A = \varepsilon cl$

A= absorbance

ε= molar absorptivity constant

c= concentration of solution

l= length of cuvette (1cm)

ε was calibrated using a 3-point average of each of the solutions seen in **Table V**.

Table V. Loading Study Standard Curve Preparation Table

Stock	Solution	Initial Concentration of AgIBU (μg/mL)	Volume of stock solution (μL)	Volume of Chloroform (μL)	Volume of DMSO (μL)	Volume total (μL)
WS	1	0	0	900	300	1200
WS	2	3.125	37.5	900	262.5	1200
WS	3	6.25	75	900	225	1200
WS	4	12.5	150	900	150	1200
WS	5	25	300	900	0	1200
IS	6	50	60	900	240	1200
IS	7	100	120	900	180	1200
IS	8	150	180	900	120	1200
IS	9	200	240	900	60	1200
IS	10	250	300	900	0	1200

Note: Initial Stock: 1mg/mL, AgIBU in DMSO. Working Stock: 100μL of IS plus 900μL DMSO.

The loading efficiency was calculated for each scaffold to determine the efficiency of AgIBU loading into PCL nanofibers using **Formula 2**.

Formula 2. Loading Efficiency $Loading\ Efficiency = \frac{Actual\ Loading\ \%}{Theoretical\ Loading\ \%}$

Release Study

The rate at which AgIBU was released from the scaffold was measured by suspending 10mg samples of AgIBU-loaded scaffolds and 10mg unloaded scaffold controls in PBSoln solution at 5mg/mL. At 12hr, 24hr, 48hr, and 72hr, 50% of the solution was extracted and frozen at -80º C. Equal volume of extracted solution was replaced with fresh PBSoln. At 84 hours, all collected samples were lyophilized for 48 hours. After lyophilization, the samples were each resuspended in 1.2 mL of 50%, v/v ACN: 50%, v/v DIW solution. The samples were centrifuged at 15,000 rpm for 5 minutes at 4ºC and absorbance values were determined at 260nm. These absorbance values were subjected to comparison with the Release Study Standard Curve in

Table VI to determine the rate of release as well as the percent-elution of total loaded drug from the scaffold in a polar solvent.

Table VI. Release Study Standard Curve Preparation Table

Solution	**Initial Concentration of AgIBU (μg/mL)**	**Stock**	**Volume of Stock solution (μL)**	**Volume of buffer solution (μL)**	**Final volume (μL)**
1	0	WS	0	1200	1200
2	3.125	WS	37.5	1162.5	1200
3	6.25	WS	75	1125	1200
4	12.5	WS	150	1050	1200
5	25	WS	300	900	1200
6	50	IS	60	1140	1200
7	100	IS	120	1080	1200
8	150	IS	180	1020	1200
9	200	IS	240	960	1200
10	250	IS	300	900	1200

Note: Buffer: 50% ACN by volume, 50% DIW by volume. IS: 1μg/mL, AgIBU in Buffer. WS: 100 μL IS, 900 μL Buffer.

In order to standardize the efficacy of drug release between scaffolds of different drug composition, the TCDR **Formula 3** was calculated and used for comparison.

Formula 3. TCDR $TCDR = LE * m * ACDR_{24}$

LE= Loading efficiency

m=total mass of scaffold (mg)

$ACDR_{24}$= Average Cumulative Drug Release at 24 hours

CHAPTER III

RESULTS

Structural Analysis of AgIBU

Silver salt of ibuprofen was synthesized with over 90% yield and characterized using mass spectrometry and H^1-NMR. AgIBU mass spectrometry characterization (**Fig. 6**) confirms ionized ibuprofen by peaks at 205.19 m/z (purple in **Fig. 6**), AgIBU by a peak at 311.28 m/z peak (green **Fig. 6**) and methylation of AgIBU by peak at 339 m/z. The mass shift associated with these peaks confirms the formation of silver ibuprofen. In addition to "mass-spec" characterization, H^1-NMR (**Fig. 7**) indicates characterization of benzene peaks at 7.1ppm (green and blue), methyl peaks at 1.0 and 1.5ppm (orange and yellow), methane peaks at 1.75 and 3.5 ppm (pink and purple). Finally, the absence of an ibuprofen carboxylic acid peak 12.8ppm (gray box) and the absence of impurities demonstrates that silver is bound to hydroxyl of ibuprofen carbonyl carbon. The DMSO solvent peak is present at 2.5ppm.

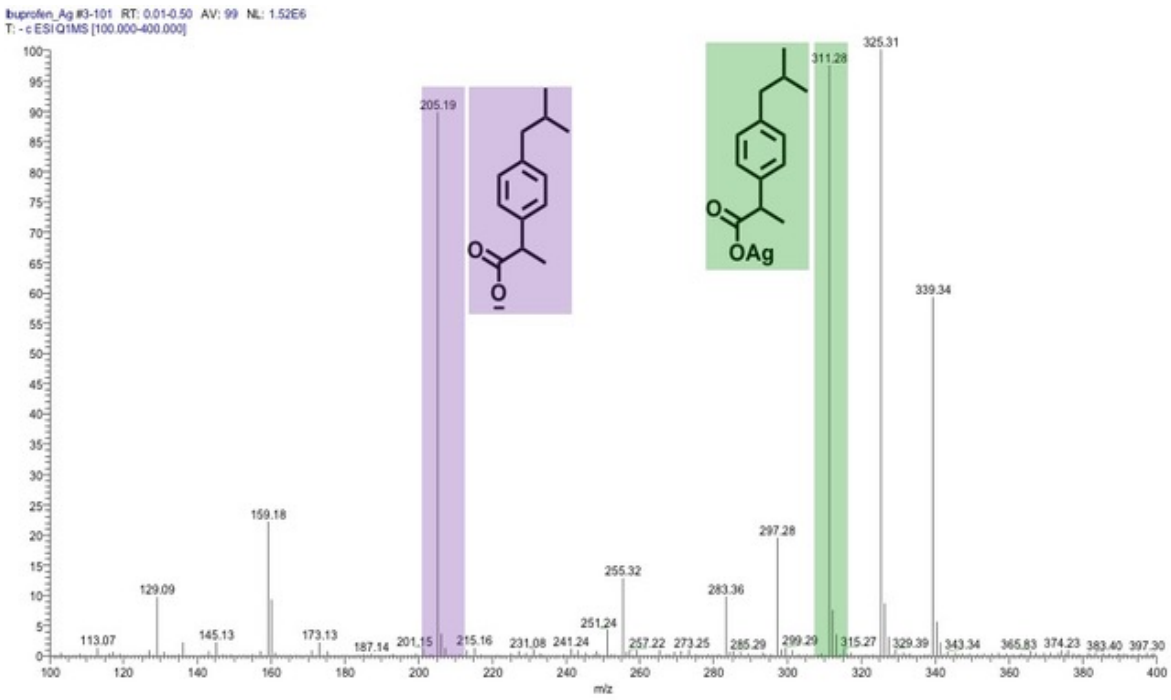

Figure 6. Mass spectrometry characterization of ionized ibuprofen (left) and ionized silver ibuprofen (right).

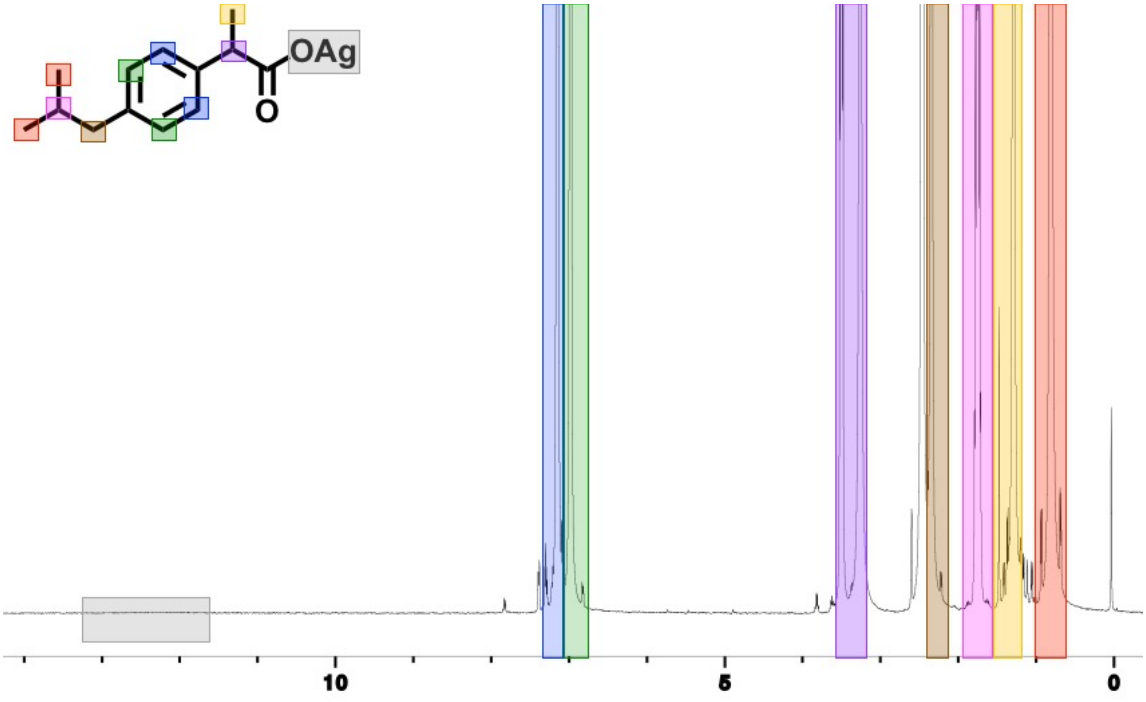

Figure 7. H^1-NMR characterization of silver ibuprofen with highlighted functional groups.

Bacterial Susceptibility

The minimum inhibitory and bacterial concentration (MIC and MBC) were used to determine the concentration of AgIBU required to inhibit growth and kill bacteria. While AgIBU resulted in the inhibition of growth in all strains tested, AgIBU was not bactericidal against all strains within the concentration range tested **(Fig. 8-10)**. The MIC of AgIBU against *P. aeruginosa* was 2-8µg/mL **(Fig. 8),** and the MBC 4-8µg/mL for all of the strains tested. *S. epidermidis (***Fig. 9)** strains were all inhibited by <8µg/mL of AgIBU, but displayed a wide range of MBC values, all of which lay in the range of concentrations tested. In contrast to these two species, many MRSA strains **(Fig. 10)** were not killed within the concentrations tested even though AgIBU inhibited the growth of all the tested strains. Nevertheless, AgIBU demonstrates significant antimicrobial activity against all three pathogens.

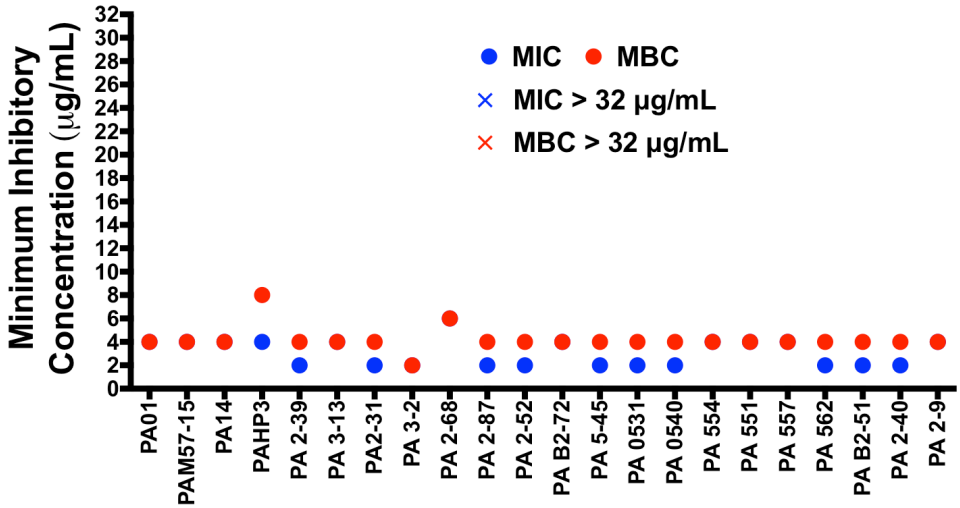

Figure 8. Minimum inhibitory and bactericidal concentration of silver ibuprofen (AgIBU) against *P. aeruginosa* exhibiting bactericidal activity.

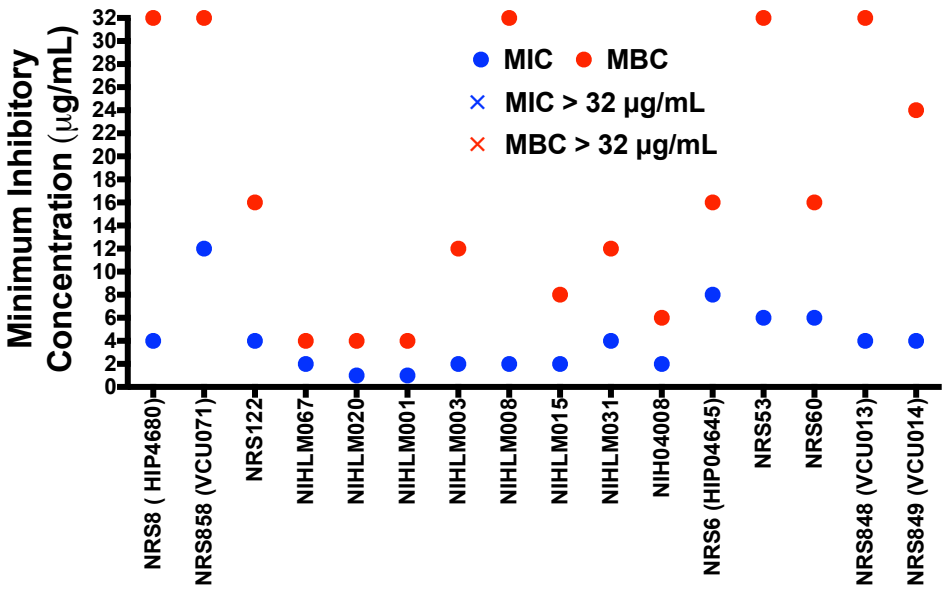

Figure 9. Minimum inhibitory and bactericidal concentration of silver ibuprofen (AgIBU) against *S. epidermidis* exhibiting inhibitory and bactericidal activity.

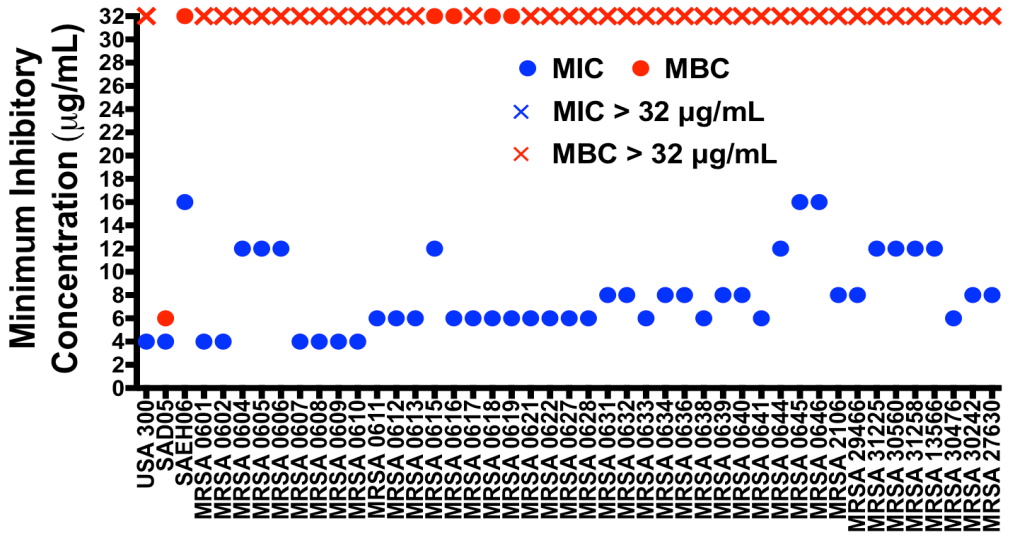

Figure 10. Minimum inhibitory and bactericidal concentration of silver ibuprofen (AgIBU) against MRSA exhibiting inhibitory activity.

SEM Characterization

SEM images of unloaded (**Fig. 11)** and AgIBU-loaded (**Fig. 12)** nanofiber scaffolds revealed the formation of nanofibers composed of PCL as well as AgIBU association with PCL. The presence of AgIBU deposits in SEM imagery served as qualitative confirmation that AgIBU can be loaded into PCL nanofibers using electrospinning.

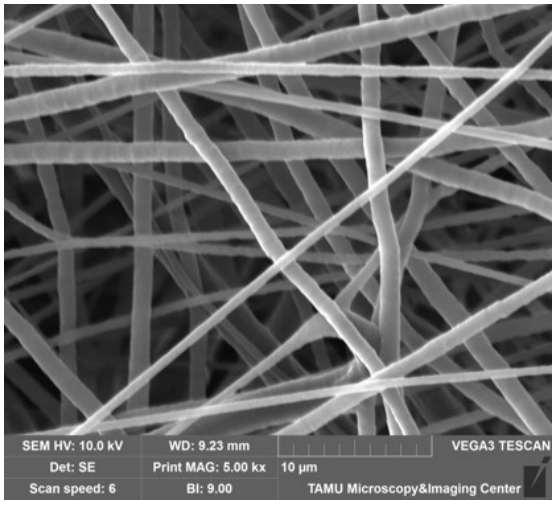

Figure 11. Unloaded scaffold SEM image displaying polycaprolactone (PCL) nanofibers.

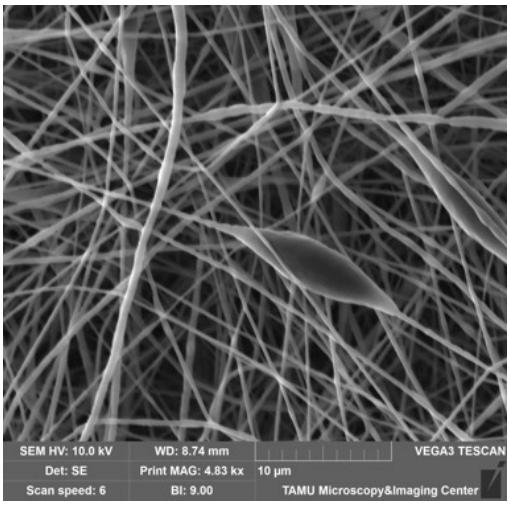

Figure 12. AgIBU-loaded scaffold SEM image displaying silver ibuprofen (AgIBU) deposits incorporated into the polycaprolactone (PCL) nanofibers.

Loading study

Quantitative evaluation of the loading capacity of PCL nanofibers for AgIBU revealed that PCL nanofibers are capable of high loading capacities and are thus excellent carriers for AgIBU. To test the effect of loading percentage on the release rate of AgIBU from the scaffolds, both 10% and 20% nanofiber scaffolds were fabricated (**Fig. 13)**. The 10% scaffold retained near 100% loading efficiency **Formula 2**, however, an apparent saturation occurred between 10% and 20% leading to a decrease in loading efficiency from near 100% to approximately 75%.

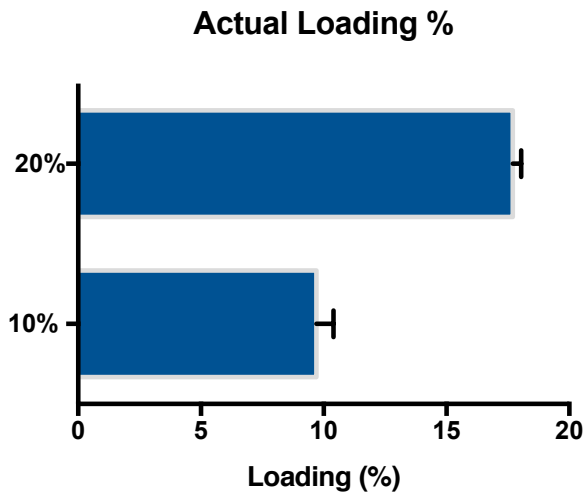

Figure 13. Loading capacity of 500mg polycaprolactone (PCL) nanofibers for silver ibuprofen AgIBU based on mass percentage.

Release study

Electrospun nanofibers composed solely of PCL displayed poor release kinetics and low at 24 hours when using 10% loaded scaffolds, correlating to a TCDR of 0.3mg at 24 hours **Formula 2**. To improve the elution rate and hence, therapeutic efficiency, 20% loaded scaffolds were used which lead to an improvement in release kinetics and an increase in ACDR, correlating to a TCDR of 13.5mg at 24 hours. When PEG, an amphiphilic compound, was

incorporated into the polymer solution of the scaffold, a massive improvement in both release kinetics and ACDR was observed, leading to a TCDR of 26mg at 24 hours (**Fig. 14)**. The improvement in release rate of AgIBU increases the possibility of attaining inhibitory and bactericidal concentrations in a timely manner allowing for the rapid treatment of SSIs. Ultimately, because these improved release kinetics improve the therapeutic utility of the scaffold, they also improve its commercial viability.

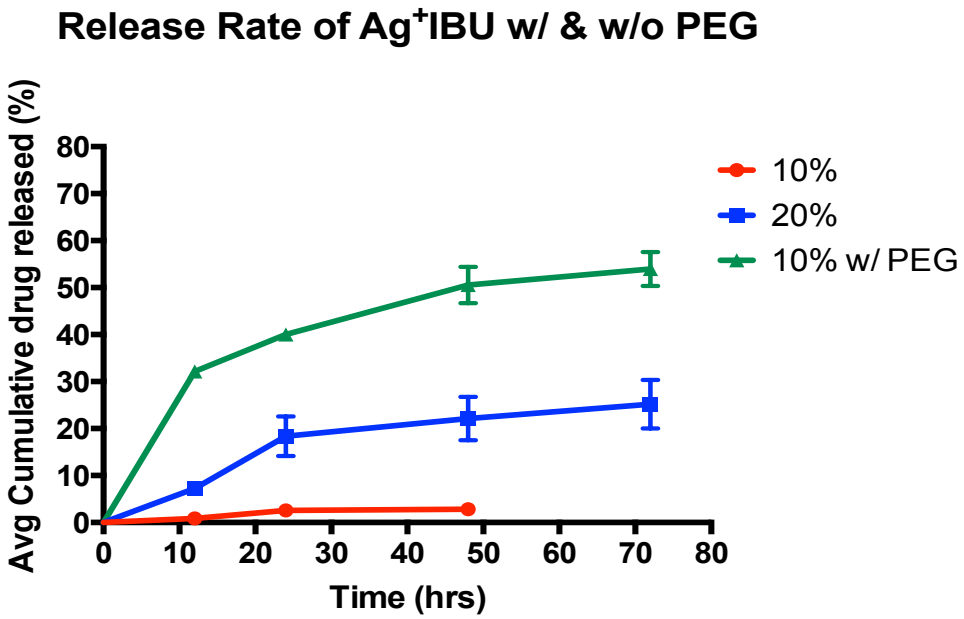

Figure 14. Release rate of silver ibuprofen (AgIBU) from 500mg nanofiber scaffolds based on mass percentage.

CHAPTER IV

DISCUSSION

We have demonstrated the synthesis of AgIBU, and confirmed its structure via mass spectroscopy and H^1-NMR. AgIBU displays potent antimicrobial efficacy against many strains of bacterial pathogens prevalent in SSIs, killing all *P. aeruginosa* at 8μg/mL and inhibiting all strains of *S. epidermidis* and MRSA at 16μg/mL. SSIs with these pathogens, *P. aeruginosa*, *S. epidermidis,* and MRSA, all result in significant morbidity for patients. Because AgIBU demonstrates efficacy against all bacterial strains tested, it holds great promise as a novel antimicrobial treatment for infections involving the skin flora. As demonstrated by R Raina, NAC is able to rescue human dermal fibroblasts (HDFs) from the metal-induced cytotoxicity of AgIBU [10]. Given NAC's ability to abrogate the metal-induced toxicity in HDFs, when used in conjunction with AgIBU, it may be possible to treat SSIs with very high concentrations of AgIBU, effectively achieving and maintaining the sterility of surgical sites.

Through the use of SEM imagery, the formation of PCL nanofibers was verified, as well as the presence of AgIBU deposits, confirming the association of AgIBU with PCL. This association was vital in displaying the nanofibers' ability to carry to AgIBU to wound sites. Loading studies quantified the efficacy of the nanofibers to carry AgIBU. These loading studies displayed that PCL nanofibers can effectively be loaded with AgIBU up until 10% mass percentage, afterwards saturation begins to occur, resulting in decreased loading efficiency. Release studies allowed for the examination of the scaffolds' ability to elute AgIBU into phosphate buffer solution. When PCL was the only polymer used to compose the nanofibers, very poor elution was achieved. To improve the release rate, an increased loading concentration

of AgIBU was tested, which improved the release rate, but still left most of the AgIBU trapped inside the scaffold. To release AgIBU deposits, the scaffold must undergo a degradation reaction involving water and the PCL shell surrounding the AgIBU deposits present in the scaffold. Due to the hydrophobicity of PCL, water cannot easily access the deposits and initiate the degradation and release of AgIBU. To improve the yield of AgIBU elution from a scaffold, a process dependent on the degradation reaction, PEG was incorporated into the polymer solution to serve as a hydrophilic component. During electrospinning, PEG associated with PCL and was incorporated into the nanofibers surrounding the AgIBU, allowing water to be more readily recruited and initiate the degradation reaction. The incorporation of PEG largely improved the elution rate and cumulative drug release into the phosphate buffer solution as verified by the release studies. The loading and release studies serve as proof-of-concept that AgIBU can not only be loaded into nanofiber scaffolds, but can also be released at concentrations significantly higher than MBC values seen in *P. aeruginosa*, *S. epidermidis,* and MRSA.

Because of AgIBU's novel capabilities to act as an anti-inflammatory and an antimicrobial, it is an ideal compound for the treatment of SSIs. Delivering the compound via nanofiber elution allows for the direct and continuous treatment of SSIs while reducing the pain at the site of incision. Using this novel therapy, SSIs may be dramatically reduced, thus further improving the safety of surgeries in the United States.

Future Experiments

Preincubation with NAC was shown to be vital in the abrogation of the cytotoxic effects of AgIBU. However, MIC/MBC experiments will need to be performed with AgIBU and NAC

together followed by determination of the Fractional Inhibitory Concentration (FIC) to determine if there are any synergistic or antagonistic effects between the two compounds *in vitro*.

It is possible that in SSIs, biofilms may be established. Given biofilms' increased resistance to antimicrobial therapies, AgIBU needs to be tested against biofilms of different pathogenic bacteria prevalent in SSIs. The minimum biofilm inhibitory concentrations will be determined and used to modify and improve the release kinetics of AgIBU from the nanofiber scaffolds to ensure bactericidal effects towards the bacteria harbored in biofilms.

Electrospun nanofibers composed of PCL and PEG exhibited an astounding ability to load and release AgIBU at concentrations significantly higher than those necessary to achieve bactericidal effects against many of the strains of bacteria tested. To further test the efficacy of nanofiber-elution therapy for the treatment of surgical site infections, studies must be performed on the simultaneous release of NAC and AgIBU. These studies will clarify how NAC must be eluted to effectively abrogate the silver-induced cytotoxicity of AgIBU.

Lastly, elution-based kill-kinetics studies must be performed to observe how fast bacteria are able to adjust to increasing concentrations of AgIBU and how this affects their MIC values. Using this data, the release properties of nanofiber scaffolds may be adjusted to achieve the minimum inhibitory and bactericidal concentrations (MIC and MBC) against a wide range of pathogens in a timely manner.

REFERENCES

1. Magill SS, Edwards JR, Bamberg W, et al. 2014. Multistate point-prevalence survey of health care-associated infections. N Engl J Med 370: 1198-1208.

2. Anderson DJ, Podgorny K, Berrios-Torres SI, et al. 2014. Strategies to Prevent Surgical Site Infections in Acute Care Hospitals: 2014 Update. Infect Control Hosp Epidemiol 35(6): 605-627.

3. Giacometti A, Cirioni O, Schimizzi A, Del Prete M, Barchiesi F, D'erricoM, Petrelli E, Scalise G. 2000. Epidemiology and Microbiology of Surgical Wound Infections. J Clin Microbiol 38(2): 918-922.

4. Fair R, Tor Y. 2014. Antibiotics and Bacterial Resistance in the 21st Century. Perspect Medicin Chem https://dx.doi.org/10.4137%2FPMC.S14459.

5. Appelbaum PC. 2012. 2012 and Beyond: Potential for the Start of a Second Pre-antibiotic Era? J Antimicrob Chemotherap 67(9): 2062-2068.

6. Jung WK, et al. 2008. Antibacterial activity and mechanism of action of the silver ion in Staphylococcus aureus and Escherichia coli. Appl Environ Microbiol 74(7): 2171-2178.

7. Dakal T, Kumar A, Majumdar R, Yadav V. 2016. Mechanistic Basis of Antimicrobial Actions of silver Nanoparticles. Front Microbiol https://doi.org/10.3389/fmicb.2016.01831.

8. Wakshlak R, Pedahzur R, Avnir D. 2015. Antibacterial Activity of Silver-killed Bacteria: The "Zombies" Effect. Sci Rep https://doi.org/10.1038/srep09555.

9. Siddiqui MA, Ahmad J, Majeed Khan MA, et al. 2012. Nickel oxide nanoparticles induce cytotoxicity, oxidative stess, and apoptosis in cultured human cells that is abrogated by the dietary antioxidant curcumin. Food Chem Toxicol 50(3): 641-647.

10. Raina R, Chirra B, Shah KN, Cannon CL. 2018. Undergraduate Thesis. Texas A&M University, College Station, TX. Silver Ibuprofen-Induced Cytotoxicty Abrogated by N-Acetyl Cysteine.

11. Konstan MW, et al. 1995. Effect of high-dose ibuprofen in patients with cystic fibrosis. N Engl J Med 332(13): 848-854.

12. Shah P, Marshall-Batty K, Smolen J, Tagaev J, Chen Q, Rodesney C, Le H, Gordon V, Greenberg D, Cannon C. 2018. Antimicrobial Activty of Ibuprofen against Cystic Fibrosis-Associated Gram-Negative Pathogens. Antimicrob Agents Chemther https://doi.org/10.1128/AAC.01574-17.

13. Nanoscience. 2018. Electrospinning. https://www.nanoscience.com/techniques/electrospin/. Cited 16 Sep 2018.

14. Kikionis S, Ioannou E, Konstantopoulou M, Roussis V. 2017. Electrospun Micro/Nanofibers as Controlled Release Systems for Phermones of Bactrocera oleae and Prays oleae. J Chem Ecol https://doi.org/10.1007/s10886-017-0831-2.

15. Weldon C, Tsui J, Shankarappa S, Nguyen V, Ma M, Anderson D, Kohane D. 2012. Electrospun Drug-Eluting Sutures for Local Anasthesia. J Control Release https://doi.org/10.1016/j.jconrel.2012.05.021.

16. Radhakrishnan J, Krishnan UM, Sethuraman S. 2014. Hydrogel Based Injectable Scaffolds for Cardiac Tissue Regeneration. Biotechnol Adv 32: 449-461.